# Static exchange and cluster modeling of core electron shakeup spectra of surface adsorbates: CO/Cu(100)

Hans Ågren, Vincenzo Carravetta, and Lars G. M. Pettersson
*Institute of Physics and Measurement Technology, Linköping University, S-58183, Linköping, Sweden; Istituto di Chimica Quantistica ed Energetica Molecolare del C.N.R., Via Risorgimento 35, 56100 Pisa, Italy; and Institute of Physics, University of Stockholm, Box 6730, S-113 85 Stockholm, Sweden*

Olav Vahtras
*Institute of Physics and Measurement Technology, Linköping University, S-58183, Linköping, Sweden*
(Received 4 December 1995)

An *ab initio* static exchange approach is devised for calculations of the core-electron shake phenomenon of large species. The approach employs appropriately spin-coupled two-hole potentials for the various shakeup/shakeoff channels. It is far extendable in the number of atoms treated, in the one-particle basis set, and in the spectral range, while restricted in correlation to full intrachannel correlation. Using cluster modeling it is implemented for shake spectra of molecules adsorbed on surfaces. A demonstration is given for the oxygen and carbon shake spectra of $COCu_N$, $N=0,14,50$, modeling CO/Cu(100). The reduction of shake energies and the accompanying increase in intensity are well recovered by the large cluster employed ($COCu_{50}$), while the small cluster ($COCu_{14}$) could only recover half the total shakeup/shakeoff intensity created by the absorption. An assignment of the strong low-lying shakeup states could be obtained in terms of orbital excitations and in terms of local versus delocalized characters of these excitations. Results for the oxygen and carbon shakeup spectra of free carbon monoxide are analyzed in some detail in view of data from high-resolution experiments and from other theoretical approaches.

## I. INTRODUCTION

Unlike many other phenomena associated with core-electron spectroscopies, there has been a widening gap between experiment and theory in the description of the core-electron shake phenomenon. New dimensions to shakeup spectroscopy have been added by tunable synchrotron excitation and by new types of samples. For about two decades the studied samples have also included surface-adsorbed species.[1] Shakeup spectra of such species show some salient features compared to the free-molecular case, like characteristic lowering of the shakeup energies and strong increase of their intensities. These features are shown to be very dependent on the strength of interaction between the surface and the adsorbate and have been proposed to be used to characterize the interaction.

The theoretical investigations of shakeup spectra from surface-adsorbed species, still relatively few in number, have utilized both solid state and molecular modeling. These models interpret the spectra using different vocabularies and are not in complete agreement with each other. In the present work we adopt the molecular standpoint and approach the surface-adsorbate system by cluster modeling, starting from the free molecule and considering larger clusters that might reach the properties of the macroscopic system. As shown in many articles, this has constituted a viable proposition for ground-state properties as well as for spectroscopy. More recent applications, relating to the technique we adopt in the present work, have also concerned core-electron spectroscopies, viz., x-ray emission[2] (XES) and near-edge x-ray absorption fine-structure[3] (NEXAFS) spectroscopies. Due to the intrinsic complexity of the shakeup process and the lack of consensus in its interpretation, it is, however, not evident that a cluster model provides a reasonable approach also for shakeup spectra of surface adsorbates. The goal of this work is therefore twofold; to devise and test a direct static exchange cluster method for shakeup, and to attempt an assignment of shake spectra of a particular adsorbate. Our choice falls on the CO/Cu(100) system partly because of previous experience of modeling this system, but also because this system is representative for most aspects of shakeup of surface adsorbates. Furthermore, the CO molecule is of interest on its own since it has provided perhaps the best-resolved molecular shakeup spectra to date, which, in addition, appear very different for the two core sites. It belongs to the class of unsaturated molecules for which the shakeup part of the core-electron spectrum is particularly intense and rich in structure.

In the following section, Sec. II, we present the computational model in some detail since in several aspects it constitutes a different technique for shakeup/shakeoff analysis, and give computational details of the present work. In Sec. III A we present the results for the free CO molecule, and compare these with experiment and briefly also with previous computational approaches for this molecule. Section III B presents the results for oxygen and carbon shake spectra for two clusters; $COCu_{14}$ and $COCu_{50}$. A final discussion of the results is given in the last section, Sec. IV.

## II. METHOD AND CALCULATIONS

### A. Basic approximations

We confine ourselves to excitation energies and intensities with respect to the shake phenomenon in the limit of

 

high energies, and ignore fine structures and effects due to vibronic coupling, angular distributions, or finite lifetimes, etc. We use a set of approximations for the photoexcitation process, sometimes collectively called the ''sudden approximation,'' namely, (i) dipole transitions in an N-electron system according to Fermi's golden rule; (ii) strong-orthogonality approximation for the outgoing photoelectron; (iii) neglect of conjugate transitions; (iv) neglect of hole mixing; and (v) neglect of variation of the photoelectron matrix elements. Further approximation levels can then be referred to computations rather than to modeling (i.e., final- and initial-state correlation, self-consistent descriptions, etc.). A discussion of the role of these approximation schemes for the analysis of shakeup (models and computations) can be found in Refs. 4 and 5; the original mathematical formulations can be found in papers by Martin and Shirley[6] (first quantization) and by Arneberg, Müller, and Mann[7] (second quantization).

At level (iii) given above the intensity is expressed as

$$I_{f\epsilon}=\left|\sum_i T_{i\epsilon}G_i\right|^2, \tag{1}$$

where we denote $T_{i\epsilon}$ as the orbital element

$$T_{i\epsilon}=\langle\phi_\epsilon|\hat{t}|\phi_i\rangle \tag{2}$$

and $G_i$ as the generalized overlap amplitude

$$G_i=\langle\Psi_f^{N-1}|\hat{a}_i|\Psi_{\text{g.s.}}^N\rangle. \tag{3}$$

Here $\Psi_{\text{g.s.}}$ and $\Psi_f^{N-1}$ are the ground-state and the final-ionic-state wave functions, respectively, $\hat{a}_i$ the annihilation operator for the ground state, and $\hat{t}$ the one-electron dipole operator. The continuum orbital describing the photoelectron is denoted $\phi_\epsilon$ and $\phi_i$ is a molecular orbital of the initial state. In the approximation level (iv) we take into account that the core orbitals are nearly orthogonal to any other orbital and therefore that *hole-mixing* effects of primary core photoelectron channels can safely be neglected. This means that the summation in Eq. (1) can be reduced to the contribution of a single core hole, $i=x$. This leads to approximation (v) for high-energy excitation, since, with only one $T_{x\epsilon}$ element left, its absolute value is of no consequence for the shakeup analysis provided it does not vary over the narrow energy interval for $\epsilon$ covered by the shake spectrum.

### B. Static exchange approximation

The expression given in Eq. (1) with the restriction of $i=x$ thus follows from the Fermi golden rule in the dipole approximation, with a strong-orthogonality condition for the outgoing photoelectron:

$$\Psi_{f\epsilon}^N=\Psi_f^{N-1}\otimes\phi_\epsilon. \tag{4}$$

The photoelectron moves in the potential of the N-1 electrons, which are not assumed to correlate with the photoelectron, i.e., the ion is frozen (static) with respect to the interaction with the excited electron, but full exchange in this interaction is accounted for [static exchange approximation (STEX)]. In this approximation the final state of the molecular excitation process is described by the promotion of an electron from an occupied orbital to a virtual orbital that is an eigenvector of a Hamiltonian describing the motion of the excited electron in the electrostatic field of the remaining molecular ion. In the present work we adopt a static exchange approximation also for the *secondary*, shake, electron excitation. This approximation, which previously was formulated by the authors for molecular shakeoff continua,[11] assumes that the shake electron motion is defined by the N-2 potential and that a shakeup/shakeoff state is expressed as

$$\Psi_f^{N-1}=\Psi_f^{N-2}\otimes\phi'_{\epsilon'}, \tag{5}$$

where the secondary shakeup/shakeoff electron function $\phi'_{\epsilon'}$ is strongly orthogonal to the remainder N-2 electron state $\Psi_f^{N-2}$ and determined variationally in the field of the two-hole ion:

$$\hat{\mathscr{H}}^{N-2}|\phi'_{\epsilon'}\rangle=\epsilon'|\phi'_{\epsilon'}\rangle. \tag{6}$$

We construct one static exchange Hamiltonian $\hat{\mathscr{H}}^{N-2}$ for each shake channel defined by the primary ionization orbital $x$, by the secondary ionization (or excitation) orbital $j$, and by the particular spin coupling $S$. For a closed-shell ground state and nondegenerate orbitals $x$ and $j$, the static exchange Hamiltonian has the following general expression:

$$\hat{\mathscr{H}}_{x,j,S}^{N-2}=\hat{F}+c_{J_x}\hat{J}_x+c_{K_x}\hat{K}_x+c_{J_j}\hat{J}_j+c_{K_j}\hat{K}_j, \tag{7}$$

where the coupling coefficients $c_J$ and $c_K$ depend on the adopted coupling scheme (see Table I). Here $\hat{F}$ is the standard Fock operator for double occupancy of the orbitals and $\hat{J}$ and $\hat{K}$ are the usual Coulomb and exchange operators; the molecular orbitals building up this static exchange Hamiltonian are obtained by an optimization for the $x$th hole. If there are open shells in the ground state the correction to the closed-shell Fock operator is obtained by adding $\hat{J}$ and $\hat{K}$ operators in Eq. (7) corresponding to the open shells, and multiplied by the coupling coefficients for the spin coupling in question. A useful approximation for the ''passive'' open shells is the high-spin approximation, which can be accommodated here by a summation with additional coupling coefficients $c_J=-1$ and $c_K=\frac{1}{2}$; neglecting the spin coupling of these open shells with the orbitals $x$ and $j$.

TABLE I. Coupling coefficients for different shake channels.

| Ionization orbital | Primary | | Secondary | |
|---|---|---|---|---|
| Coupling coefficient | $c_J$ | $c_K$ | $c_J$ | $c_K$ |
| Case 1 [a] | −1.0 | 0.5 | −1.0 | 0.5 |
| Case 2 [b] | −1.0 | 1.5 | −1.0 | 1.5 |
| Case 3 [c] | −1.0 | 0.5 | −1.0 | 2.0 |
| Case 4 [d] | −1.0 | 1.5 | −1.0 | 0.0 |

[a]Singlet coupling of primary (core) and secondary (shake) orbitals first.

[b]Triplet coupling of primary (core) and secondary (shake) orbitals first.

[c]Singlet coupling of secondary (shake) and excited (STEX) orbitals first.

[d]Triplet coupling of secondary (shake) and excited (STEX) orbitals first.

The excitation energies of the shake spectrum are obtained by adding the second ionization potential (shakeoff threshold), for each given shake channel $IP_{xjS}^{N-2}=E_{xjS}^{N-2}-E_{\mathrm{g.s.}}^{N}$, to the eigenvalues of the STEX matrix, while the corresponding transition moments are obtained as monopole matrix elements between ground state and STEX final states projected on mutually nonorthogonal sets of molecular orbitals. Thus the vertical shake transition energy is defined as $w_{xjS}(\epsilon')=\epsilon'+IP_{njS}^{N-2}$ and the eigenpairs $[w_{xjS}(\epsilon'),I_{xjS}(\epsilon')]$, where $I_{xjS}(\epsilon')=|\langle\Psi_{xjS\epsilon'}^{N-1}|\hat{a}_x|\Psi_{\mathrm{g.s.}}^{N}\rangle|^2$ form true representations of shakeup energies and intensities, respectively, in the discrete part of the spectrum where $\epsilon'<0$, while for $\epsilon'>0$ each pair $[w,I]$ forms a primitive excitation energy and intensity factor for the continuous part of the shake spectrum. This primitive spectrum of order $M$ is converted, by the Stieltjes imaging procedure, to a quadrature spectrum of order $n$ ($n\ll M$) such that the first $2n$ spectral moments are reproduced.[9,10] From this quadrature spectrum the final, so-called Stieltjes-imaged photoionization cross sections can be obtained as described in Ref. 11.

The spin-coupling coefficients are derived from expectation values of the $(N-1)$-electron Hamiltonian over the open-shell configuration state functions (CSF's), i.e., the least linear combination of determinants that fulfill spin and spatial symmetry (monopole selection rule) for the final state, using the standard Slater-Condon rules. Each ordered spin-coupling sequence defines a CSF with a specific energy and a specific STEX Hamiltonian. The coupling order matters since CSF's obtained by different coupling orders are interacting over the Hamiltonian. We have considered two possible spin-coupling schemes for the three open-shell orbitals, core, valence, and virtual (STEX) orbitals. Both schemes generate two linearly independent final doublet states, corresponding to singlet or triplet intermediate coupling, respectively. In the first scheme (''hole'' coupling) the core and the valence orbitals are coupled first to singlet or triplet and then the coupling to the virtual orbital is considered; in the second scheme (''excitation'' coupling) we couple first the valence and the virtual orbitals (again to singlet or triplet) and then the core orbital.

In certain cases the ''excitation'' coupling can be motivated, e.g., when the virtual orbital has a strong valence character; however the ''hole'' coupling is generally the more reasonable one, as we further show here. In the STEX approximation the sums of intensities for the two coupling orders are equal. The spin-coupling coefficients for the two considered coupling schemes are given for closed-shell ground-state systems in Table I.

### C. Direct implementation

Using atomic orbital (AO) direct algorithms the usual Fock and associated static exchange matrices can be determined directly from one- and two-electron integrals computed in the atomic orbital basis. In a direct approach one uses an atomic orbital representation in which the STEX Hamiltonian matrix can be constructed directly as

$$\mathscr{H}_{ab}^{xjS}=h_{ab}+\sum_{cd}\left[2(ab|cd)DC_{cd}^{xjS}-(ac|bd)DX_{cd}^{xjS}\right] \tag{8}$$

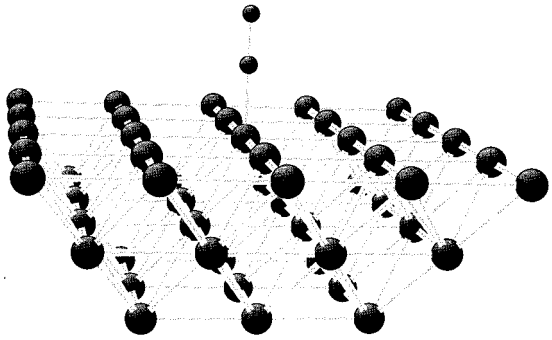

FIG. 1. Structure of the $COCu_{50}$ cluster. CO is adsorbed with the carbon end down.

by modifying the density corresponding to double occupancy according to

$$DC_{cd}^{xjS}=D_{cd}+\frac{c_{J_x}}{2}v_{cx}v_{dx}+\frac{c_{J_j}}{2}v_{cj}v_{dj}, \tag{9}$$

$$DX_{cd}^{xjS}=D_{cd}-c_{J_x}v_{cx}v_{dx}-c_{J_j}v_{cj}v_{dj}. \tag{10}$$

As for the static exchange Hamiltonian in Eq. (7), $x$ and $j$ have the meaning of primary and secondary hole shells, respectively $v_{ck}$ is component $c$ in molecular orbital $k$, $h_{ab}$ and $(ab|cd)$ denote one- and two-electron integrals, and $D$ is the density matrix in the atomic basis, corresponding to double occupancy of the orbitals. For open-shell ground states the additional $J$ and $K$ elements referring to the ground-state open orbitals can easily be introduced, as discussed in the Sec. II C, by further modification of the density. As in direct self-consistent field (SCF) calculations, the integrals are never externally stored and the density can be used to screen small elements, facts that make applications on large species possible.

### D. Cluster modeling

The calculations have been performed using clusters modeling on-top chemisorption of CO at the Cu(100) surface (Fig. 1). The Cu atom to which the CO molecule binds is treated at the all-electron level, while the rest of the cluster atoms are described by one-electron effective core potentials (ECP's).[12] For free CO the experimental geometry was used, while for the clusters the results from geometry optimization were adopted. This optimization was performed using density-functional theory[13–16] for the $Cu_{13}CO$ system with an all-electron Cu atom surrounded by nine-electron ECP's (i.e., valence consisting of $3s, 3p$, and $4s$). In the one-electron ECP model[12] the core (including the $3d$ shell) is described by a static potential, which includes the effects of relaxation and polarization of the $3d$ orbitals, but which only treats the $4sp$ valence electrons explicitly. The basis set used is a $(4s1p)$ primitive basis contracted to $[2s1p]$.[12] The directly interacting ''all-electron'' copper atom is described by the Wachters[17] basis set extended with two diffuse $p$ and one diffuse $d$ functions). For adsorbed and free CO we used a TZPD (triple-$\zeta$ plus polarizing and diffuse functions) basis set.[18] In addition, the molecular basis was augmented with a large (141 functions) diffuse basis centered at the site of the

TABLE II. Carbon 1*s* and oxygen 1*s* main line intensities and ionization potentials (IP's) (eV) for $COCu_M$, $N=0,14,50$

| Complex | C 1*s* IP | C 1*s* Intens. | O 1*s* IP | O 1*s* Intens. |
|---|---|---|---|---|
| CO | 297.41 | 0.800 | 542.07 | 0.741 |
| $COCu_{14}$ | 296.04 | 0.578 | 539.81 | 0.550 |
| $COCu_{50}$ | 293.05 | 0.286 | 537.41 | 0.279 |

core hole. This basis was generated by adding 19*s*, 19*p*, and 19*d* functions with exponents obtained by an even-tempered scaling, $\alpha_n=\alpha_0\beta^{-n}$, with $\alpha_0=1.238a_0^{-2}$ and $\beta=1.4$; the smallest exponent used was $0.0029a_0^{-2}$. The same augmentation basis was used for both carbon and oxygen in the construction of the STEX matrices. The present parametrization of the $COCu_N$ clusters has been extensively tested previously both for general applications[19] and in calculations of x-ray absorption[20] and emission spectra.[2] The structure of the $COCu_{50}$ cluster is displayed in Fig. 1. See also Table II.

### E. Computations

There are six basic steps in static exchange shakeup calculations (compare with the corresponding calculations of x-ray absorption spectra in Ref. 21): (1) direct self-consistent field (SCF) and ΔSCF wave-function optimizations; (2) computation of modified densities and the STEX Hamiltonian; (3) augmentation with a very large and diffuse basis set and transformation of the STEX Hamiltonian $(1-P)\mathscr{H}^{i,j,S}(1-P)$, where P projects out the occupied orbitals; (4) diagonalization to obtain eigenvalues and eigenvectors; (5) computation of overlap amplitudes with the ground state; (6) Stieltjes imaging for the shake-off part of the spectrum.

Note that in comparison with the SCF or ΔSCF optimization all other steps are computationally cheap, in particular the construction of the STEX matrix. The static exchange method[21] devised here not only is applicable to large systems, but also can be applied to calculate a wide portion of the core excitation spectrum, for shake structures both below and above the ionization limit. The basis set augmentation leads to close-to-full basis set results (without having to optimize the wave functions in the full basis).

Since the STEX eigenvalues are defined only with respect to the ionization limits, here the secondary, shakeoff, limits $E_f^{i,j,S}$, these must be precomputed. We use an algorithm which is in parity with the computation of the potential:

$$E_f^{i,j,S}=\Delta E_{\mathrm{SCF}}-\epsilon_j+\begin{cases}2(ij|ji) & \text{for singlet coupling}\\ 0 & \text{for triplet coupling,}\end{cases} \tag{11}$$

where $\epsilon_j$ is the orbital energy of the secondary hole orbital and $(ij|ji)$ is the exchange integral involving the two hole orbitals. This means that the shakeoff edges (and therefore the reference level for the shake spectra) are fully relaxed with respect to the creation of the first (core) hole, but frozen with respect to the creation of the second (valence) hole (but with correct core-valence spin coupling). From experience with primary photoionization, we expect this actually to be a better proposition than separate ΔSCF's, because pure non-interacting, spectroscopic states are obtained (and because relaxation and correlation errors will partly cancel). The present STEX algorithm has been implemented in the direct SCF program DISCO,[22] which is also used as the underlying electronic structure code.

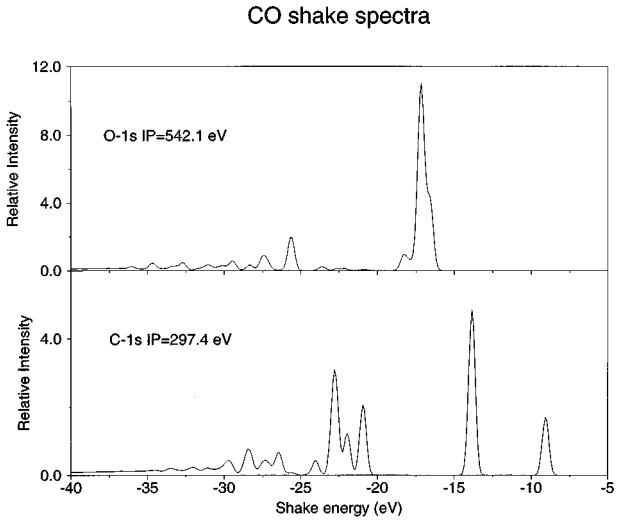


FIG. 2. Computed O 1*s* and C 1*s* shake spectra for gas-phase CO.

## III. RESULTS AND DISCUSSION

### A. Carbon monoxide

Although the present computational scheme focuses on large, and in this work surface-adsorbed species, it is instructive first to see how it performs for the free CO molecule. Carbon monoxide forms a suitable first test for the STEX algorithm also because it shows very well-resolved shake spectra. The assignment of these spectra is still not settled despite having been the object of several previous investigations. The results for the total and individual channel shake spectra for CO, oxygen and carbon, are presented in Figs. 2 and 3, respectively. We have focused in these figures on the strong $5\sigma$, $1\pi$, and $4\sigma$ channels; computations for the $3\sigma$ channel show it to be both weak and high in energy. The experimental core ionization spectra of CO show details up to 40 eV in the shake region. The high-resolution recordings[23] reveal that the oxygen and carbon spectra are remarkably different in appearance. In the former, the intensity peaks are collected in the 15–20 eV interval, while in the carbon spectrum there are many intensive peaks spread in the 10–25 eV interval. The STEX calculation allows a detailed assignment of most of these features.

The first experimental[23] carbon peak (8.34 eV, intensity 2.3% can be straightforwardly assigned to the singlet-hole coupled $\pi$-$\pi^*$ excitation [9.04 eV, 1.7%]. Likewise, the second peak is assigned as the triplet-hole coupled $\pi$-$\pi^*$ excitation (14.88 eV, 4.8%) compared to [13.84 eV, 4.8%] (here and in the following we prefer to use for the hole-coupling scheme). The corresponding oxygen peaks are grouped together at (15.9 eV, 11.2%), while the STEX calculations predict [16.56 eV, 4.1%] and [17.14 eV, 10.9%] for the singlet-hole and triplet-hole coupled $\pi$-$\pi^*$ excitations, respectively. It is also notable that these single-excitation tran-

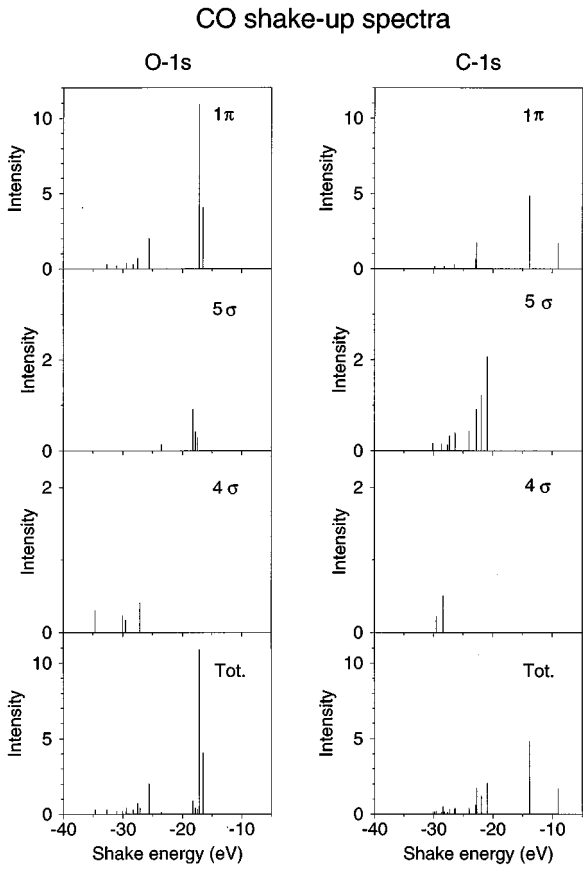


FIG. 3. Computed O 1*s* and C 1*s* separate-channel spectra for gas-phase CO.

sitions are stronger in the oxygen than in the carbon spectrum, which can probably be related to the larger orbital relaxation energies for O 1*s* ionization.

The next group of states, which we assign as due to $\sigma$ excitations, falls quite close on the high-energy side of the $\pi$-$\pi^*$ excitations in the oxygen spectrum, while they are somewhat more spread in the carbon spectrum. The weak double-peak feature at 18 eV in the oxygen spectrum is thus assigned to the different-hole-coupled O $1s^{-1}5\sigma^{-1}6\sigma^{1}$ configuration states. The very weak peak around 20 eV (''5'' in Ref. 23) seems to be without counterpart in the STEX scheme, and originates therefore as an almost pure double excitation. The remaining peaks up to about 30 eV are due to higher shake transitions from the $1\pi$ and $5\sigma$ orbitals. The onset for the $4\sigma$ transitions resides at 27 eV (at features ''8'' and ''9'' of Ref. 23), thus beyond the double-ionization threshold of the $5\sigma$ channel; see Table III.

The calculations seem to recapitulate the positions and intensities of higher excitations in the oxygen spectrum quite well, while their positions in the carbon spectra are pushed up in energy by a few eV. Thus the highly resolved peaks ''3''–''8'' between 18 and 23 eV in the carbon shake spectrum,[23] must be attributed to the computed peaks between 20 and 25 eV with similar magnitudes of intensity. As in the oxygen spectrum, these higher discrete transitions are due to several high shake transitions from the $1\pi$ and $5\sigma$ orbitals; see Figs. 2 and 3. We take this shift as an indication of the role of double excitations in the carbon spectrum, as predicted for a few states by previous configuration-

TABLE III. Carbon 1*s* and oxygen 1*s* shakeup energies (eV) and intensities (arbitrary units) for CO.

| Transition | Energy | Intensity |
|---|---|---|
| | C spectrum | |
| Main peak | 0.0 | 1.0 |
| $1\pi$(S) | −9.04 | 0.0171 |
| $1\pi$(S) | −22.94 | 0.0065 |
| $1\pi$(S) SOT [a] | −31.21 | |
| $5\sigma$(S) | −22.71 | 0.0092 |
| $5\sigma$(S) | −24.01 | 0.0044 |
| $5\sigma$(S) | −28.66 | 0.0016 |
| $5\sigma$(S)SOT | −32.77 | |
| $4\omega$(S) | −29.53 | 0.0022 |
| $4\sigma$(S)SOT | −37.25 | |
| $3\sigma$(S)SOT | −57.78 | |
| $1\pi$(T) | −13.84 | 0.0485 |
| $1\pi$(T) | −22.75 | 0.0175 |
| $1\pi$(T) | −26.52 | 0.0032 |
| $1\pi$(T) | −28.19 | 0.0016 |
| $1\pi$(T) | −29.85 | 0.0019 |
| $1\pi$(T)SOT | −30.59 | |
| $5\sigma$(T) | −20.92 | 0.0207 |
| $5\sigma$(T) | −21.96 | 0.0122 |
| $5\sigma$(T) | −26.36 | 0.0040 |
| $5\sigma$(T) | −27.28 | 0.0033 |
| $5\sigma$(T) | −27.64 | 0.0015 |
| $5\sigma$(T) | −30.10 | 0.0017 |
| $5\sigma$(T) SOT | −30.14 | |
| $4\sigma$(T) | −28.39 | 0.0051 |
| $4\sigma$(T) SOT | −35.73 | |
| $3\sigma$(T) SOT | −56.26 | |
| | O spectrum | |
| Main peak | 0.0 | 1.0 |
| $5\sigma$(S) | −17.83 | 0.0043 |
| $5\sigma$(S) SOT | −26.67 | |
| $1\pi$(S) | −16.56 | 0.0409 |
| $1\pi$(S) | −27.48 | 0.0071 |
| $1\pi$(S) SOT | −35.70 | |
| $4\sigma$(S) | −29.52 | 0.0018 |
| $4\sigma$(S) SOT | −40.15 | |
| $3\sigma$(S) | −51.42 | 0.0016 |
| $3\sigma$(S) SOT | −62.13 | |
| $5\sigma$(T) | −17.45 | 0.0031 |
| $5\sigma$(T) | −18.27 | 0.0090 |
| $5\sigma$(T) | −23.54 | 0.0015 |
| $5\sigma$(T) SOT | −26.41 | |
| $1\pi$(T) | −17.14 | 0.1089 |
| $1\pi$(T) | −25.61 | 0.0202 |
| $1\pi$(T) | −28.31 | 0.0031 |
| $1\pi$(T) | −29.40 | 0.0040 |
| $1\pi$(T) | −31.07 | 0.0021 |
| $1\pi$(T) | −32.66 | 0.0031 |
| $1\pi$(T) SOT | −33.50 | |
| $4\sigma$(T) | −27.17 | 0.0040 |
| $4\sigma$(T) | −30.04 | 0.0024 |
| $4\sigma$(T) | −34.65 | 0.0030 |
| $4\sigma$(T) SOT | −37.31 | |
| $3\sigma$(T) | −47.66 | 0.0025 |
| $3\sigma$(T) SOT | −57.69 | |

[a]Shakeoff threshold.

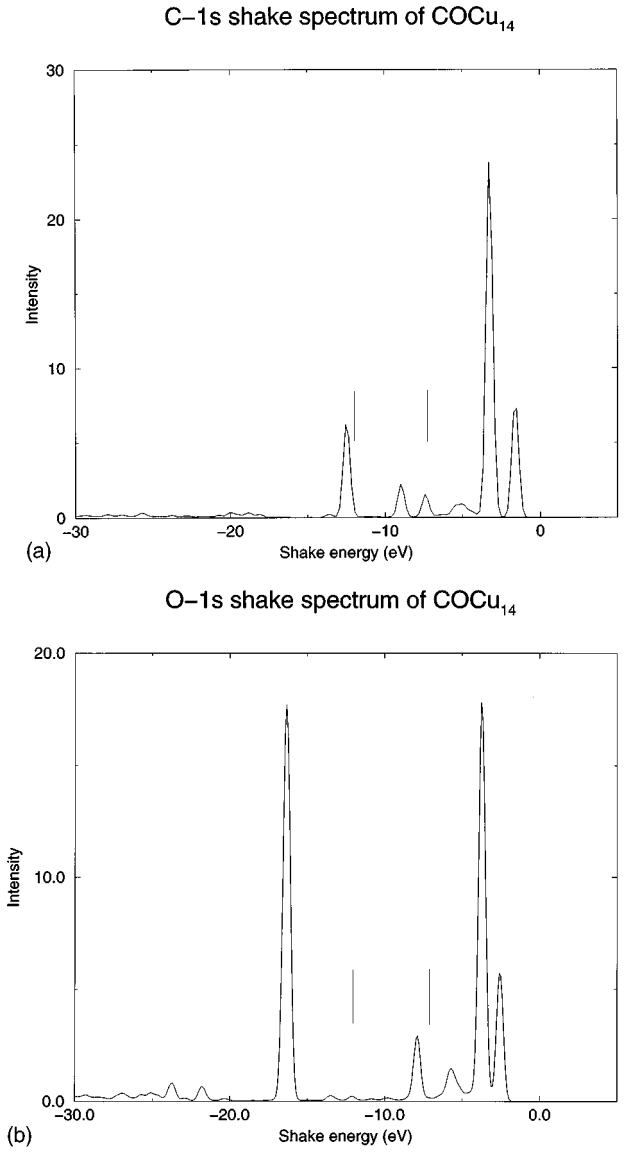


FIG. 4. Computed C 1*s* and O 1*s* shake spectra for $COCu_{14}$. (a) Carbon spectrum. (b) Oxygen spectrum. The two bars indicate the $\sigma$ and $\pi$ channel shakeoff thresholds. The intensity is normalized to the intensity of the main state (not shown).

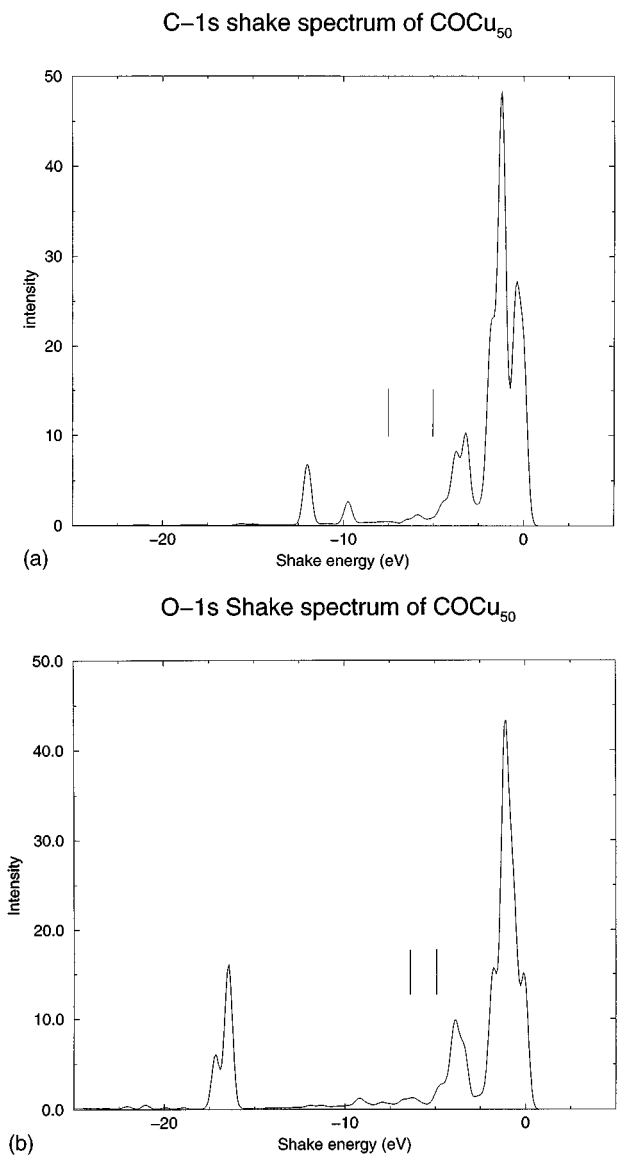


FIG. 5. Computed C 1*s* and O 1*s* shake spectra for $COCu_{50}$. (a) Carbon spectrum. (b) Oxygen spectrum. The two bars indicate the $\sigma$ and $\pi$ channel shakeoff thresholds. The intensity is normalized to the intensity of the main state (not shown).

interaction (CI) calculations.[24] It is noteworthy that their intensities are still correct in magnitude. The $4\sigma$ transitions are high in energy also in the carbon spectrum, being responsible for much of the diffuse structure close to 30 eV.

The shake spectra shown in Fig. 2 account also for a portion, ca. 20 eV, of the continuum. As seen in the figure these shakeoff, parts of the shake channels are very weak. It is known that atomic shake spectra often show open-channel (Feshbach) resonances,[25] but it has been questioned whether molecules develop closed-channel (shape) resonances in their shake spectra[26] in analogy with shape resonances in primary photoionization. It is therefore interesting to note that for intensive shakeup spectra, like those of CO, the near-edge shakeoff parts are still weak with no trace of resonances. The weaker ''bumps'' still observed in the continuous spectra should be attributed to discrete states embedded in the continuum, here mostly the $4\sigma$ states embedded in the continua of the $5\sigma$ and $1\pi$ shake channels. Within the adopted single-channel approach we do not obtain the proper ''smearing'' effect of such embeddings.

Considering that the shake spectra of CO have been regarded as notoriously difficult, the present calculations manage to recapitulate them remarkably well. The unsaturated character of CO with a relatively low-lying valencelike orbital induces an increased role of correlation for the discrete shakeup peaks. Thus Guest *et al.*,[24] using a selection-CI technique, characterized only the two first carbon shakeup peaks as single excitations ($\pi^{-1}$-$\pi^{*1}$), while the next three were assigned considerable double-excitation character ($\pi^{-2}$-$\pi^{*2}$ and $\sigma^{-2}$-$\pi^{*2}$). Multiconfiguration (MC) SCF calculations by the present authors[27,11] also attribute some double-excitation character to the second $\pi$-$\pi^*$ peak. For unsaturated systems, double excitations may become energetically possible also between valencelike levels, e.g., $\pi$ and $\pi^*$ levels, in the presence of a core hole. This can ac-

TABLE IV. Carbon 1*s* shakeup energies (eV) and intensities for $COCu_{14}$.

| Transition | Energy | Intensity |
|---|---|---|
| | Singlet-hole coupling | |
| $\pi_0$ | 1.62 | 0.078 |
| $\pi_{-1}$ | 4.93 | 0.006 |
| $\sigma_{-2}$ | 5.07 | 0.002 |
| $\pi_{-2}$ | 8.97 | 0.022 |
| | Triplet-hole coupling | |
| $\pi_0$ | 3.26 | 0.242 |
| $\sigma_{-2}$ | 4.45 | 0.003 |
| $\sigma_{-2}$ | 5.52 | 0.006 |
| $\pi_{-1}$ | 7.40 | 0.014 |
| $\sigma_{-5}$ | 12.41 | 0.002 |
| $\pi_{-2}$ | 12.48 | 0.062 |
| $\sigma_{-5}$ | 13.63 | 0.002 |
| $\sigma_{-8}$ | 19.98 | 0.003 |

centuate the initial-state correlation effect since for a closed-shell system double excitations dominate over the single excitations from the ground-state Hartree-Fock determinant; from this point of view the results of the STEX calculations for the higher-lying shakeup peaks are surprisingly good. We can only explain this fact by assuming that some of the double-excitation character of shakeup states in previous work derives from the use of basis sets too limited in size. This is also supported by the results from various CI excitation schemes (see, e.g., Ref. 28); using limited basis sets they converge to excitation energies that are several eV too large even for the first few strong shakeup peaks. In the ''ADC4'' technique[23] one starts out from ground-state orbitals and picks up relaxation by higher-order expansions of the Green's function. This procedure wrongly assigns the stronger intensity up to 20 eV as $\sigma$ excitations with the first intensive $\pi$ excitation residing at 21.67 eV.[23] We can also establish that the missing ''triplet $\pi$-$\pi^*$'' transition in the oxygen spectrum is not due to weak or zero intensity,[23,29] but due to accidental overlap with the ''singlet $\pi$-$\pi^*$'' transi-

TABLE V. Oxygen 1*s* shakeup energies (eV) and intensities for $COCu_{14}$.

| Transition | Energy | Intensity |
|---|---|---|
| | Singlet-hole coupling | |
| $\pi_0$ | 2.58 | 0.058 |
| $\pi_{-1}$ | 5.82 | 0.010 |
| $\pi_{-2}$ | 16.45 | 0.050 |
| | Triplet-hole coupling | |
| $\pi_0$ | 3.73 | 0.174 |
| $\sigma_{-2}$ | 5.42 | 0.002 |
| $\sigma_{-3}$ | 5.54 | 0.005 |
| $\pi_{-1}$ | 7.91 | 0.028 |
| $\sigma_{-5}$ | 13.55 | 0.002 |
| $\pi_{-2}$ | 16.29 | 0.136 |
| $\pi_{-2}$ | 21.84 | 0.006 |
| $\pi_{-2}$ | 23.71 | 0.006 |

TABLE VI. Carbon 1*s* shakeup energies (eV) and intensities for $COCu_{50}$.

| Transition | Energy | Intensity |
|---|---|---|
| | Singlet-hole coupling | |
| $\sigma_0$ | −0.05 | 0.048 |
| $\pi_0$ | 0.46 | 0.235 |
| $\pi_{-1}$ | 1.54 | 0.026 |
| $\pi_{-2}$ | 3.13 | 0.022 |
| $\pi_{-7}$ | 9.74 | 0.025 |
| | Triplet-hole coupling | |
| $\sigma_0$ | −0.05 | 0.142 |
| $\pi_0$ | 1.21 | 0.461 |
| $\pi_0$ | 1.80 | 0.129 |
| $\pi_0$ | 2.24 | 0.016 |
| $\pi_0$ | 3.22 | 0.074 |
| $\pi_0$ | 3.74 | 0.021 |
| $\pi_0$ | 4.32 | 0.009 |
| $\pi_{-1}$ | 1.85 | 0.073 |
| $\pi_{-1}$ | 2.67 | 0.011 |
| $\pi_{-1}$ | 4.02 | 0.014 |
| $\pi_{-2}$ | 3.75 | 0.046 |
| $\pi_{-2}$ | 4.56 | 0.012 |
| $\pi_{-2}$ | 5.94 | 0.008 |
| $\pi_{-7}$ | 11.99 | 0.067 |

TABLE VII. Oxygen 1*s* shakeup energies (eV) and intensities for $COCu_{50}$.

| Transition | Energy | Intensity |
|---|---|---|
| | Singlet-hole coupling | |
| $\sigma_0$ | 0.04 | 0.037 |
| $\pi_0$ | 0.63 | 0.178 |
| $\pi_{-1}$ | 1.58 | 0.015 |
| $\pi_{-1}$ | 1.66 | 0.014 |
| $\pi_{-2}$ | 3.35 | 0.035 |
| $\pi_{-7}$ | 17.15 | 0.059 |
| | Triplet-hole coupling | |
| $\sigma_0$ | 0.08 | 0.111 |
| $\pi_0$ | 0.82 | 0.071 |
| $\pi_0$ | 1.15 | 0.385 |
| $\pi_0$ | 1.81 | 0.050 |
| $\pi_0$ | 2.31 | 0.010 |
| $\pi_0$ | 3.39 | 0.017 |
| $\pi_0$ | 3.99 | 0.013 |
| $\pi_{-1}$ | 1.65 | 0.011 |
| $\pi_{-1}$ | 1.84 | 0.070 |
| $\pi_{-1}$ | 4.32 | 0.009 |
| $\pi_{-2}$ | 3.66 | 0.028 |
| $\pi_{-2}$ | 3.93 | 0.062 |
| $\pi_{-2}$ | 4.75 | 0.014 |
| $\pi_{-6}$ | 9.19 | 0.008 |
| $\pi_{-7}$ | 16.42 | 0.160 |

TABLE VIII. Character of $\pi$ orbitals in C $1s^{-1}$ state of $COCu_{50}$ important for the shake spectrum.

| Atom [a] | $1m$ | $\pi_{-7}$ | $\pi_{-6}$ | $\pi_{-2}$ | $\pi_{-1}$ | $\pi_{0}$ | $\pi_{+1}$ | $\pi_{+2}$ |
|---|---|---|---|---|---|---|---|---|
| Occup. | | 2.00 | 2.00 | 2.00 | 2.00 | 2.00 | 0.00 | 0.00 |
| Energy | | −0.73 | −0.60 | −0.35 | −0.27 | −0.24 | −0.12 | −0.12 |
| C | $P_{010}$ | −0.78 | −0.06 | −0.24 | 0.17 | −0.46 | −0.36 | 0.39 |
| C | $P_{010}$ | 0.15 | 0.02 | 0.04 | −0.03 | 0.06 | 0.05 | −0.04 |
| C | $P_{010}$ | 0.18 | 0.04 | −0.05 | 0.00 | 0.01 | 0.01 | −0.12 |
| C | $P_{010}$ | −0.02 | −0.05 | −0.14 | 0.03 | −0.03 | −0.18 | −0.68 |
| C | $D_{011}$ | −0.02 | −0.02 | 0.01 | 0.00 | 0.01 | 0.00 | 0.00 |
| C | $D_{011}$ | 0.00 | −0.02 | 0.02 | −0.01 | 0.03 | 0.02 | −0.03 |
| C | $D_{011}$ | 0.04 | −0.04 | 0.01 | −0.01 | 0.00 | −0.02 | 0.00 |
| O | $P_{010}$ | −0.66 | −0.27 | 0.24 | −0.12 | 0.31 | 0.23 | −0.22 |
| O | $P_{010}$ | −0.01 | 0.00 | 0.00 | 0.00 | 0.00 | 0.00 | 0.00 |
| O | $P_{010}$ | −0.01 | 0.00 | 0.04 | −0.02 | 0.05 | 0.03 | −0.01 |
| O | $P_{010}$ | −0.02 | 0.02 | 0.04 | −0.03 | 0.11 | 0.16 | 0.00 |
| O | $D_{0.01}$ | 0.01 | 0.00 | 0.00 | 0.00 | 0.00 | 0.00 | 0.00 |
| O | $D_{011}$ | 0.04 | 0.01 | 0.00 | 0.00 | 0.00 | 0.00 | 0.00 |
| O | $D_{011}$ | 0.01 | 0.01 | 0.00 | 0.00 | 0.01 | 0.01 | −0.03 |
| Cu | $P_{010}$ | −0.01 | 0.00 | −0.02 | 0.01 | −0.02 | −0.01 | 0.01 |
| Cu | $P_{010}$ | 0.02 | 0.01 | 0.07 | −0.03 | 0.06 | 0.02 | −0.03 |
| Cu | $P_{010}$ | −0.01 | −0.05 | −0.15 | 0.04 | −0.11 | −0.02 | −0.01 |
| Cu | $P_{010}$ | 0.04 | 0.09 | 0.69 | −0.02 | −0.54 | −0.29 | 2.92 |
| Cu | $D_{011}$ | −0.18 | 0.70 | 0.02 | −0.01 | 0.09 | 0.09 | −0.08 |
| Cu | $D_{011}$ | −0.10 | 0.38 | 0.01 | −0.01 | 0.05 | 0.05 | −0.04 |
| Cu | $D_{011}$ | −0.01 | 0.05 | 0.01 | 0.001 | −0.01 | −0.01 | 0.01 |

[a]Copper atom binding to CO.

tion. A complete active-space MCSCF calculation of the type given in Refs. 27 and 11 recapitulates the two first peaks well, with somewhat too high energy, but seems to overestimate the role of higher-order excitations in the wave function.

### B. Carbon monoxide adsorbed on copper

#### *1. Spectral character*

The most striking difference between the shake spectra of free CO and of CO/Cu(100) is the intense low-lying shake feature residing 2 eV above the main line.[30] A second feature is discerned about 3 eV further up in the spectra. The relative intensity of the main line is considerably reduced, and the distinction between ''main'' and ''satellite'' peaks is no longer obvious. From being very different in character the oxygen and carbon spectra have become very much alike for the CO/Cu(100) system.[30]

The computational results for the carbon and oxygen shake spectra of the $COCu_{14}$ and $COCu_{50}$ clusters are shown in Figs. 4 and 5 and in Tables IV, V, VI, and VII. The first strong peak, which in both intensity and energy is in good agreement with experiment, has developed already for $COCu_{14}$, but its intensity is still increased by more than a factor of 2 in both spectra when going from $COCu_{14}$ to $COCu_{50}$. The second salient peak seems to be even more dependent on the cluster size; it increases in intensity and decreases in energy going from $COCu_{14}$ to $COCu_{50}$; its intensity seems still to be somewhat underestimated with respect to experiment.[30] A third intensive feature has developed at large excitation energies, embedded in the continua of very many shake channels. We find strong similarity between the carbon and oxygen spectra, which indeed is the case in the experimental recording.[30]

The computational results indicate that both the oxygen and carbon shake spectra are sparse. Only few channels are active, and in each such channel there are only few excitations that provide intensity to the shake spectrum. Counting transitions with more then 5% of the main peak, the shakeup spectra of $COCu_{50}$ (carbon and oxygen) are made up from one triplet-hole-coupled transition from the lowest $\sigma$ orbital [highest occupied molecular orbital (HOMO)], three excitations from the $\pi$ orbital ($\pi_0$) with the lowest binding energy, and one each from the $\pi_{-1}$, $\pi_{-2}$, and $\pi_{-7}$ orbitals ($\pi_{-n}$ is the $n$th $\pi$ orbital counting from $\pi_0$). To this one should add the singlet-hole-coupled counterpart of the second $\pi_0$ transition which contributes by 20% of the main peak intensity. The two coupling schemes certainly give the asymmetry of the strongest shake feature in these spectra. The present results indicate that the role of this exchange-induced splitting, which so far has been an open question for surface-adsorbate spectra, is considerably reduced with respect to free CO, from several eV to within an eV. It is, however, still a factor to be considered for the adsorbate spectra. For higher shake excitations from a given occupied orbital, the splitting seems to be reduced and the differently spin-coupled shakeoff thresholds become almost degenerate.

The remaining strong shakeup feature in the discrete part resides at about 4 eV from the main peak and is due to a shake transition from the $\pi_{-2}$ orbital. The third feature far up in the continuum is the feature which differs most between the carbon and oxygen spectra. The explanation of this curiosity can be found in the fact that the orbital responsible

TABLE IX. Gross atomic charge and overlap populations for ground state and carbon and oxygen 1*s* core-hole states of CO and $COCu_{50}$.

| State | C | O | Cu |
|---|---|---|---|
| | CO | | |
| Ground State | | | |
| C | 5.773 | | |
| O | 0.625 | 8.227 | |
| C 1*s* state | | | |
| C | 5.408 | | |
| O | 0.385 | 7.592 | |
| O 1*s* state | | | |
| C | 5.110 | | |
| O | 0.276 | 7.890 | |
| | $COCu_{50}$ | | |
| Ground state | | | |
| C | 5.941 | | |
| O | −1.821 | 8.533 | |
| Cu | 1.037 | −2.113 | 24.250 |
| C 1*s* state | | | |
| C | 6.346 | | |
| O | −2.216 | 8.413 | |
| Cu | 1.262 | −2.837 | 24.462 |
| O 1*s* state | | | |
| C | 6.157 | | |
| O | −2.721 | 8.298 | |
| Cu | 1.436 | −2.681 | 24.540 |

for this high shake transition, the $\pi_{-7}$ orbital, is very much like the $1\pi$ orbital of free CO. Thus the energy and intensity character of this $\pi$-$\pi^*$ transition are largely preserved on going from free CO to $COCu_{50}$. In contrast to the low-lying transitions which have no counterparts in free CO, this transition retains much of the free CO character, including the differences between the oxygen and carbon spectra. As shown in Ref. 30, the intensity at 10–15 eV is a common feature in the spectra of CO adsorbed on Cu, Ni, and Ag. This supports its interpretation as an intermolecular transition. Since it interacts with multiple continua one can expect a considerable smearing of this structure (which would be obtained in a full coupled-channel approach), which might be a factor responsible for the observed intensity in the shakeoff tail.[30] As for free CO, no channel shows a trace of ''shape'' resonant behavior (closed-channel resonances).

The remaining salient feature to be accounted for is the first low-lying $\sigma_0$ transition residing just at the main transition, the only intensive transition in the $\sigma$ manifold of orbitals. As seen in Table VI it even receives a small negative shake energy in the carbon spectrum. We find that $\sigma_0$ is almost a pure cluster orbital in the ground state, (see also Table X); it finds some amplitude on the carbon site for both core-hole states. This type of low-lying shake transition can only appear as a broadening of the main band, and can probably be seen as an analogue to the Doniach-Sunjic-type hole-pair excitations[31] describing the asymmetrization of the core photoelectron lines in solids. We do not, however, take the negative shake energy literally as a signature of a shakedown process. Shakedown seems to be an intrinsic notion of ground-state models (either Green's function[32,33] or the solid state model Hamiltonians[34–36]) while separate state optimization of orbitals and configurations generally gives positive ''shake'' energies.[37] In the STEX procedure we use separately optimized core strate orbitals to construct the potential, but with shake energies related to the ionization limit, here the second ionization limit (or shakeoff threshold), which thus might end up slightly below the first ionization limit for shake transitions with very small energies.

The addition of the strongest shake transitions amounts to a considerable integrated shakeup/shakeoff intensity in the spectra. The computed squared overlap amplitudes for the main carbon and oxygen core-hole states are as low as 0.29 (C 1*s*) and 0.28 (O 1*s*)., These numbers accord with inspection of the experimental spectra,[30] and can be compared to the corresponding measured values of 0.29 (O 1*s*) and 0.36 (O 1*s*) for the CO/Ni(100) system.[38] It is interesting to note that the $COCu_{14}$ system is only halfway between CO and $COCu_{50}$ with respect to the main state overlap amplitudes; 0.80-0.56-0.29 for C 1*s* and 0.74-0.55-0.28 for O 1*s*. These figures thus indicate that clusters of the size $COCu_{14}$ can only account for (at most) half of the integrated shakeup/shakeoff intensity induced by the presence of the copper surface.

#### *2. Orbital contributions and screening*

Much of the earlier modeling of surface-adsorbed shake spectra has focused on the CO/Cu(100) system. A comprehensive review of theory and experiment for this and related systems was recently given by Tillborg, Nilsson, and Mårtensson,[30] and we refer to this article for the historical account. The solid state calculations utilize two- or three-state models based on model Hamiltonians, with the surface-adsorbate interaction described by a single parameter.[34–36] The cluster approaches assign specific excitations with localization character. Transition-metal carbonyls[39] and small clusters[40,41] have served as intermediate, semiempirical, models of the solid state and molecular models; higher-level *ab initio* approaches have concerned the COCu species[42] and certain charge-transfer compounds[37] simulating some properties of the surface adsorbate.

The position and intensity of the different photoelectron structures have commonly been described by their screened or unscreened characters. The ground-state surface metal-$\pi^*$ interaction takes place mainly with CO as acceptor and metal-$\sigma$ and metal-$1\pi$ interactions mainly with CO as donor. The interactions give ''extra'' orbitals of low energy, which, although they have small carbon and especially, oxygen populations and large metal character, are important for the shake process of the surface-adsorbate system. In the core ionized states these orbitals change character substantially since they are active in the screening of the core hole, and become much more localized to the COCu system, Cu being the bonding copper atom. We have collected the most important orbitals in the $\pi$ manifold for the C $1s^{-1}$ state of $COCu_{50}$ in Table VIII, including the $\pi_{-7}$, $\pi_{-6}$, $\pi_{-2}$, $\pi_{-1}$, $\pi_0$, $\pi_{+1}$, and $\pi_{+2}$ orbitals. The first orbital level, $\pi_{-7}$, is simply the bonding $1\pi$ level of

TABLE X. Gross atomic populations for ground state and carbon and oxygen 1*s* core-hole and shakeup state orbitals of $COCu_{50}$. Orbital populations are normalized to 1.000.

| State | C s/p | C d | O s/p | O d | Cu s/p [a] | Cu d | CO tot. | Cu tot. | Cluster tot. [b] |
|---|---|---|---|---|---|---|---|---|---|
| | | | | | Ground state | | | | |
| $\sigma_0$ | | 0.017 | | −0.001 | | 0.012 | 0.016 | 0.012 | 0.972 |
| $\pi_o$ | 0.019 | 0.001 | 0.003 | | 0.011 | | 0.023 | 0.011 | 0.966 |
| $\pi_{-1}$ | 0.007 | | 0.001 | | −0.012 | −0.001 | 0.008 | −0.013 | 1.005 |
| $\pi_{-2}$ | 0.098 | 0.007 | 0.007 | −0.001 | −0.313 | | 0.111 | −0.313 | 1.212 |
| $\pi_{-7}$ | 0.246 | 0.002 | 0.649 | 0.009 | 0.004 | 0.091 | 0.906 | 0.095 | −0.001 |
| | | | | | O 1*s* state | | | | |
| $\sigma_0$ | | 0.001 | | | | −0.001 | 0.001 | −0.001 | 1.000 |
| $\pi_0$ | 0.131 | −0.002 | −0.004 | 0.002 | 0.064 | 0.011 | 0.127 | 0.075 | 0.798 |
| $\pi_{-1}$ | 0.041 | −0.001 | | 0.001 | 0.016 | 0.001 | 0.041 | 0.017 | 0.942 |
| $\pi_{-2}$ | 0.195 | 0.002 | −0.001 | −0.001 | −0.252 | 0.002 | 0.195 | −0.250 | 1.055 |
| $\pi_{-7}$ | 0.077 | −0.022 | 0.917 | 0.005 | 0.007 | 0.002 | 0.967 | 0.009 | 0.034 |
| | | | | | C 1*s* state | | | | |
| $\sigma_0$ | 0.027 | | −0.005 | | 0.029 | | 0.022 | 0.029 | 0.949 |
| $\pi_0$ | 0.130 | 0.007 | 0.079 | 0.003 | 0.050 | 0.011 | 0.219 | 0.061 | 0.720 |
| $\pi_{-1}$ | 0.019 | 0.003 | 0.012 | | 0.006 | −0.034 | 0.006 | 0.960 | |
| $\pi_{-2}$ | 0.122 | 0.009 | 0.045 | | −0.218 | | 0.176 | −0.218 | 1.042 |
| $\pi_{-7}$ | 0.388 | −0.004 | 0.550 | 0.012 | −0.005 | 0.065 | 0.946 | 0.060 | −0.006 |
| | | | | | O 1*s* shake states | | | | |
| $\sigma_0$ | 0.199 | 0.001 | −0.016 | −0.002 | 0.028 | −0.001 | 0.182 | 0.27 | 0.791 |
| $\pi_0$ | 0.156 | 0.000 | −0.020 | 0.000 | −0.198 | 0.000 | 0.136 | −0.198 | 1.062 |
| $\pi_0$ | 0.046 | −0.005 | 0.125 | 0.009 | 0.125 | 0.009 | 0.173 | 0.134 | 0.693 |
| $\pi_0$ | 0.094 | −0.008 | −0.030 | 0.001 | 0.164 | 0.015 | 0.057 | 0.179 | 0.764 |
| $\pi_{-2}$ | 0.152 | 0.000 | −0.018 | 0.000 | −0.181 | 0.001 | 0.134 | −0.046 | 0.912 |
| $\pi_{-2}$ | 0.053 | −0.005 | 0.002 | 0.001 | 0.109 | 0.009 | 0.051 | 0.169 | 0.780 |
| $\pi_{-7}$ | 0.124 | −0.001 | 0.027 | 0.001 | 0.099 | 0.011 | 0.151 | 0.161 | 0.688 |
| | | | | | C 1*s* shake states | | | | |
| $\sigma_0$ | 0.194 | 0.001 | −0.019 | −0.001 | 0.031 | −0.001 | 0.175 | 0.030 | 0.795 |
| $\pi_0$ | 0.119 | −0.002 | 0.019 | 0.001 | 0.057 | 0.005 | 0.137 | 0.062 | 0.801 |
| $\pi_0$ | 0.066 | −0.003 | 0.004 | 0.004 | 0.105 | 0.006 | 0.171 | 0.111 | 0.718 |
| $\pi_0$ | 0.195 | −0.004 | −0.047 | 0.002 | −0.015 | 0.012 | 0.146 | −0.003 | 0.857 |
| $\pi_{-1}$ | 0.067 | −0.003 | 0.000 | −0.001 | 0.098 | 0.007 | 0.063 | 0.105 | 0.832 |
| $\pi_{-1}$ | 0.089 | −0.004 | −0.014 | 0.003 | 0.111 | 0.009 | 0.074 | 0.120 | 0.806 |
| $\pi_{-2}$ | 0.179 | 0.000 | −0.025 | −0.001 | −0.217 | 0.001 | 0.153 | −0.216 | 1.063 |
| $\pi_{-2}$ | 0.048 | −0.003 | 0.009 | 0.002 | 0.137 | 0.007 | 0.056 | 0.144 | 0.800 |
| $\pi_{-7}$ | 0.112 | −0.002 | 0.021 | 0.001 | 0.101 | 0.005 | 0.132 | 0.106 | 0.762 |

[a]Copper atom binding to CO.

[b]Cluster includes all copper atoms except the one binding to CO.

free CO. It is almost completely localized to the CO adsorbate, and has about the same relative C and O character as in free CO. As noted above, it is responsible for the free-CO-like shake structures high in energy in the $COCu_{50}$ spectra. The second $\pi$ level, $\pi_{-6}$, is very much a copper 3*d* orbital, with little contribution from CO or from other copper atoms; the part which belongs to CO is still free-CO-like but localizes even more to oxygen. The third, fourth, and fifth shake-active $\pi$ levels, $\pi_{-2}$, $\pi_{-1}$, and $\pi_0$, are all internally CO antibonding $2\pi$-like levels; two of them, $\pi_{-2}$ and $\pi_0$, have large contributions on the central copper atom, while the $\pi_{-1}$ level is more delocalized over the cluster. The $\pi_{-2}$ and $\pi_0$ levels, which thus are responsible for the major part of the low-energy shake intensity, are clearly bonding (antibonding) with respect to the copper surface. The localization of these orbitals, which can be identified as the ''$\pi_b$''- and ''$\pi_a$''-type orbitals of Freund *et al.*,[39] has been disputed to some extent.[41] We find them to be of similar localization, with some more Cu *p* character at the expense of C 2*p* character for the $\pi_{-2}$ ($\pi_b$) orbital. It can be noted that the first two unoccupied $\pi$ orbitals have the same structure, internally CO antibonding and antibonding with the central

copper atom. The second of these, which is the acceptor of the strong shake transition from both the $\pi_0$ ($\pi_a$) and $\pi_{-2}$ ($\pi_b$) level, has large amplitude on the central copper atom. These strong shake transitions can in this sense be interpreted as antiscreening.

We have also collected some relevant population data in Tables IX and X. The gross atomic charge data show the substantial screening of the O 1*s* and, in particular, the C 1*s* hole states in $COCu_{50}$. The local screening is increased by 0.4 and 0.9 electron charges, respectively, compared to the corresponding core-hole states in free CO. The population data of the excited shake (''STEX'') orbitals, (see Table X), indicate strong cluster character of all these orbitals and quite small variations between the shake states. For the total screening character of the shake states, one must realize that in the construction of the spectra by the STEX procedure the screening of the core hole is separated from the population of the exited state (the potential for the shake spectrum is obtained from the fully relaxed core-hole-state orbitals). In ''reality'' screening and population are processes that are correlated to each other.

## IV. SUMMARY

We have proposed a static exchange algorithm to compute shakeup/shakeoff spectra, and used shake spectra of the CO molecule and $COCu_N$ clusters to evaluate its performance. In addition to being extendable in size, the static exchange algorithm has the comparative advantages of using correctly spin-coupled potentials, of reaching the one-particle limit (close to complete basis sets), and of covering a large portion of the energy interval including the shakeoff continuum. This should be weighed against the limited, yet well-defined, electron correlation accounted for, namely, full *intrachannel* correlation, excluding correlation that describes *interchannel* interactions.

The application to CO led to surprisingly good results. The low dominating $\pi$-$\pi^*$ single-excitation-type transitions are well reproduced; the energy and intensity character of most of the higher excitations, including those with some presumed double-excitation character, seems still to be sufficiently well predicted to be used for assignments in terms of orbital excitations. With respect to other correlation schemes, these results must be taken as indications of the importance of computing shake spectra at the full basis set limit. The most important fact is, however, that the free-CO shake spectrum is sufficiently well represented to warrant a systematic study of the chemisorbed systems.

The cluster calculations indicate a threefold division of the spectra; very intense low-lying $\pi$ excitations [HOMO-LUMO (lowest unoccupied molecular orbital) in the $\pi$ manifold], carrying most of the shake intensity; a second region at about 4 eV with penultimate or next-to-penultimate $\pi$ excitations; a third high-energy region overlapping the continuum, characterized by intramolecular excitations that preserve the signatures of the corresponding transitions in free CO. Concerning the first strong shakeup feature, we note that exchange-induced splitting forms the shape of the band, and that at the very-low-energy end, almost overlapping the main transitions, there is intense excitation in the $\sigma$ manifold with large cluster character.

The orbitals responsible for the strong shakeup transitions could be assigned special bonding and antibonding characters, internally within CO and with the surface. A significant change of these orbitals between ground and core-hole states could be noticed, something in line with the large core-hole-induced relaxation of these systems and the accompanying large shake intensities.

We find a quite slow cluster convergence; the $COCu_{14}$ species only accounts for half the cluster-induced shakeup/shakeoff intensity covered by $COCu_{50}$. We still believe that the proposed static exchange and cluster approach shows promise for investigating complicated problems such as shakeup in surface adsorbates and we foresee its application to a variety of surface-adsorbed species.

## ACKNOWLEDGMENTS

This work was carried out with support under the scientific agreement between the Swedish and Italian natural science research councils (NFR and CNR).

[1] J. C. Fuggle, T. E. Madey, M. Steinkilberg, and D. Menzel, Phys. Lett. **33**, 233 (1975).
[2] V. Carravetta, L. G. M. Pettersson, H. Ågren, and O. Vahtras (unpublished).
[3] L. G. M. Pettersson, H. Ågren, O. Vahtras, and V. Carravetta, J. Chem. Phys. **103**, 8713 (1995).
[4] H. Ågren and V. Carravetta, Int. J. Quantum Chem. **42**, 685 (1992).
[5] D. Nordfors, A. Nilsson, S. Svensson, N. Mårtensson, U. Gelius, and H. Ågren, J. Electron Spectrosc. Relat. Phenom. **56**, 117 (1991).
[6] R. L. Martin and D. A. Shirley, J. Chem. Phys. **64**, 3685 (1976).
[7] R. Arneberg, J. Müller, and R. Manne, Chem. Phys. **64**, 249 (1982).
[8] H. Ågren and H. J. Aa. Jensen, Chem. Phys. Lett. **137**, 431 (1987).
[9] P. W. Langhoff, in *Electron Molecule and Photon Molecule Collisions*, edited by T. N. Rescigno, B. V. McKoy, and B. Schneider (Plenum, New York, 1979), p. 183.
[10] P. W. Langhoff, in *Theory and Application of Moment Methods in Many-Fermion Systems*, edited by B. J. Dalton, S. M. Grimes, J. P. Vary, and S. A. Williams (Plenum, New York, 1980), p. 191.
[11] H. Ågren and V. Carravetta, J. Chem. Phys. **87**, 370 (1987).
[12] A. Mattsson, I. Panas, P. Siegbahn, U. Wahlgren, and H. Åkeby, Phys. Rev. B **36**, 7389 (1987).
[13] J. P. Perdew and Y. Wang, Phys. Rev. B **33**, 8800 (1986).
[14] J. P. Perdew, Phys. Rev. B **34**, 7406 (1986).
[15] A. St-Amant and D. R. Salahub, Chem. Phys. Lett. **169**, 387 (1990).
[16] D. R. Salahub, R. Fournier, P. Mlynarski, I. Papai, A. St-Amant, and J. Ushio, in *Density Functional Methods in Chemistry*, ed-

ited by J. Labanowski and J. Andzelm (Springer, New York, 1991), p. 77; A. St-Amant, Ph.D. thesis, Université de Montréal, 1992. The present version of the program has been substantially modified by L. G. M. Pettersson.
[17] A. J. H. Wachters, J. Chem. Phys. **52**, 1033 (1970).
[18] R. A. Kendall, T. H. Dunning, Jr., and R. J. Harrison, J. Chem. Phys. **96**, 6796 (1992).
[19] U. Wahlgren and P. E. M. Siegbahn, in *Metal-ligand Interactions: From Atoms, to Clusters, to Surfaces*, edited by D. Salahub (Kluwer, Dordrecht, 1991).
[20] L. G. M. Pettersson, H. Ågren, O. Vahtras, and V. Carravetta (unpublished).
[21] H. Ågren, V. Carravetta, O. Vahtras, and L. G. M. Pettersson, Chem. Phys. Lett. **222**, 75 (1994).
[22] J. Almlöf, K. Faegri, Jr., and K. Korsell, J. Comput. Chem. **3**, 385 (1982).
[23] J. Schirmer, G. Angonoa, S. Svensson, D. Nordfors, and U. Gelius, J. Phys. B **20**, 6031 (1987).
[24] M. F. Guest, W. R. Rodwell, T. Darko, I. Hillier, and J. Kendrick, J. Chem. Phys. **66**, 5447 (1977).
[25] S. Svensson, N. Mårtensson, and U. Gelius, Phys. Rev. Lett. **58**, 2639 (1987).
[26] S. Svensson and H. Ågren, Chem. Phys. Lett. **205**, 387 (1993).
[27] H. Ågren (unpublished).
[28] A. Lisini, G. Fronzoni, and P. Decleva, J. Phys. B **21**, 3653 (1988).
[29] G. Angonoa, O. Walter, and J. Schirmer, J. Chem. Phys. **87**, 6789 (1987).
[30] H. Tillborg, A. Nilsson, and N. Mårtensson, J. Electron Spectrosc. Relat. Phenom. **62**, 73 (1993).
[31] S. Doniach and M. Sunjic, J. Phys. C **3**, 285 (1970).
[32] W. Domcke, L. S. Cederbaum, J. Schirmer, and W. von Niessen, Phys. Rev. Lett. **42**, 1237 (1979).
[33] W. Domcke, L. S. Cederbaum, J. Schirmer, and W. von Niessen, Chem. Phys. **39**, 149 (1979).
[34] O. Gunnarson and K. Schönhammer, Solid State Commun. **26**, 147 (1978).
[35] O. Gunnarsson and K. Schönhammer, Phys. Rev. Lett. **41**, 1608 (1978).
[36] B. Gumhalter, J. Phys. C **10**, L219 (1977).
[37] H. Ågren, B. O. Roos, P. S. Bagus, U. Gelius, P. Å Malmquist, R. Maripuu, and K. Siegbahn, Chem. Phys. **77**, 3893 (1982).
[38] A. Nilsson and N. Mårtensson, Phys. Rev. B **40**, 10 249 (1989).
[39] H. J. Freund, F. Greuter, D. Heskett, and E. W. Plummer, Phys. Rev. B **28**, 1727 (1983).
[40] R. P. Messmer, S. H. Lamson, and D. R. Salahub, Solid State Commun. **36**, 265 (1980).
[41] R. P. Messmer, S. H. Lemson, and D. R. Salahub, Phys. Rev. B **25**, 3576 (1980).
[42] P. Decleva and M. Ohno, Chem. Phys. **160**, 341 (1992).